International Journal of Science and Research Archive
eISSN: 2582-8185
Cross Ref DOI: 10.30574/ijsra
Journal homepage: https://ijsra.net/

(Review Article)

Artificial Intelligence to detection fault on three phase squirrel cage induction motors subjected to stator winding fault

Balaji Dhashanamoorthi *

Master of Engineering, Control and Instrumentation, CEG, Anna University, Chennai, India.

International Journal of Science and Research Archive, 2023, 10(02), 001–015

Publication history: Received on 19 September 2023; revised on 29 October 2023; accepted on 01 November 2023

Article DOI: https://doi.org/10.30574/ijsra.2023.10.2.0859

Abstract

Induction motors are widely used in various industrial applications due to their robustness, reliability, and low cost. However, they are also prone to various types of faults, such as broken rotor bars, bearing defects, stator winding faults, and eccentricity. These faults can cause performance degradation, energy loss, and even catastrophic failures if not detected and diagnosed in time. Therefore, condition monitoring and fault diagnosis of induction motors are essential for ensuring their safe and efficient operation. In this paper, we propose a novel fault diagnosis method for induction motors based on artificial intelligence, peak variation response (PVR), park vector approach (PVA), and standard deviation (SD). The proposed method consists of four steps:

- Data acquisition and preprocessing,
- Feature extraction using pvr and pva,
- Feature selection using sd, and
- Fault classification using artificial neural networks.

The PVR and PVA are used to extract the amplitude and phase information of the stator current signals under different load conditions and fault types. The SD is used to select the most relevant features for fault diagnosis. The ANNs are used to classify the faults based on the selected features. The proposed method is validated by experimental results on a 1.5 kW three-phase induction motor with various simulated faults. The results show that the proposed method can effectively diagnose different types of faults with high accuracy and robustness.

Keywords: Fault Detection on squirrel cage induction; Park vector approach (PVA); Peak Variation Response (PVR); Standard Deviation

1. Introduction

The rotating electrical machine (motor and generator) and transformer play a vital role from small power application to large power application like power plant. The Figure 1.1 describes the basic structure of electrical system in power plant.

Wind turbines are much more expensive than diesel generators, and they also require regular maintenance that can cost up to 2% of their total price. Moreover, some parts of the wind turbines (such as blades, gearbox, tower, braking system etc.) may malfunction occasionally and increase the cost of spare and maintenance. Therefore, it is important to check the system components regularly, either by human-based resources or intelligent systems, to prevent and reduce the number of breakdowns. This leads to research opportunities in the field of condition monitoring of equipment performance and health using intelligent techniques for wind turbine systems operating in grid. By evaluating the

* Corresponding author: Balaji Dhashanamoorthi

conditions of critical system components, the faulty parts can be identified more easily and the time and maintenance cost can be reduced. Furthermore, by analyzing sensor data, implementing fault detection algorithms and using advanced signal processing, the possible faults that may occur can be predicted more accurately. The fault diagnosis of electrical machines has great benefits for both the industries and the environment. Electrical machines are suitable for developing automated equipment's. They have various applications in different fields, from power windows in automobiles to motors and transformers with tap changers used in nuclear power plants. Therefore, electrical machines have a significant role and it is essential to ensure their reliable operation. However, these electrical machines may face many faults during their life cycle. The application of condition monitoring techniques is crucial as it enables asset management, early detection of faults, prevention of severe damage and failure of electrical machines.

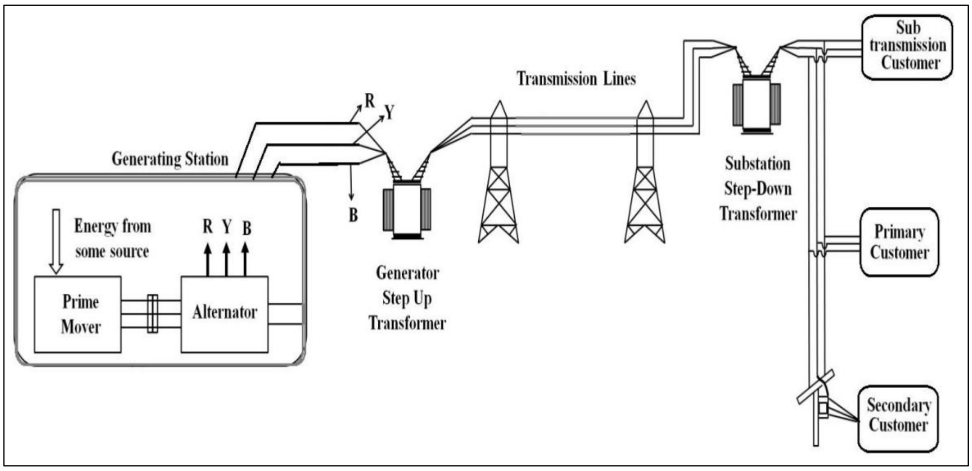

Figure 1 Basic structure of electrical system

1.1. Challenges in Electrical machines

An electrical machine component may face a challenge when its performance falls below a certain standard due to various factors such as aging, improper design, faulty installation, misuse, or a combination of these. If such a challenge is not identified and addressed in time, it may eventually lead to a breakdown. Many researchers have investigated the mechanisms of breakdowns in electrical machines and developed methods to detect them at an early stage. The common internal challenges can be divided into two types.

- Electrical Challenges.
- Mechanical Challenges.

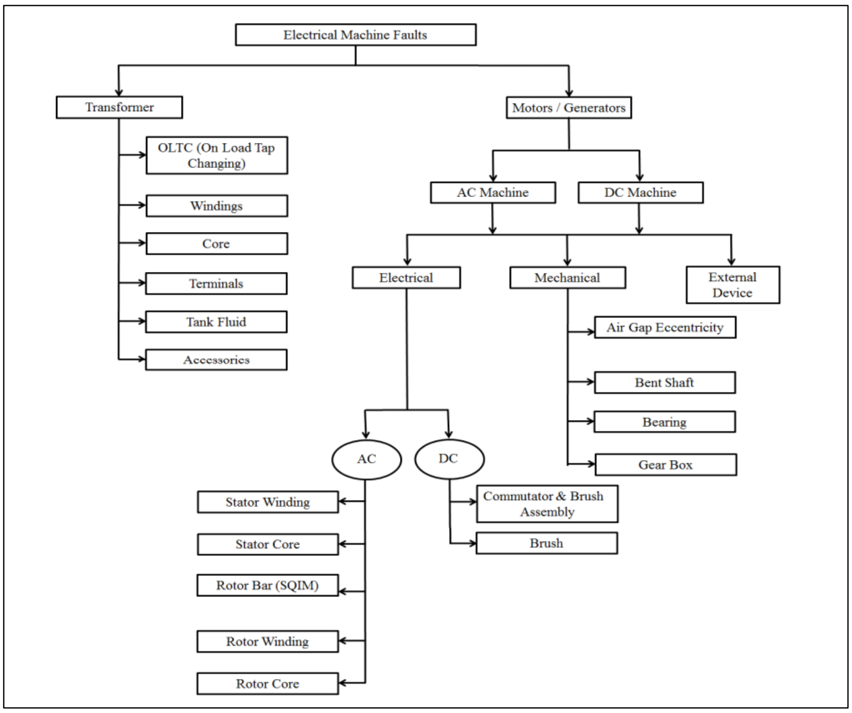

Figure 2 Tree structure representing various failures in electrical machines

1.2. Proposed Electrical Monitoring Techniques

1.2.1. Park Vector Approach (PVA)

To get the Park's vector pattern, the programming is done with signal processing module of LabVIEW software. The induction motor has been initially tested, in the absence of faults in order to determine the reference current Park's vector pattern corresponding to the supposed healthy motor. The Squirrel Cage Induction Motor (SCIM) has been modelled and simulated with unbalanced supply and turn dislocation of pole. The data has been analyzed by Park Vector Approach and compared with the healthy pattern.

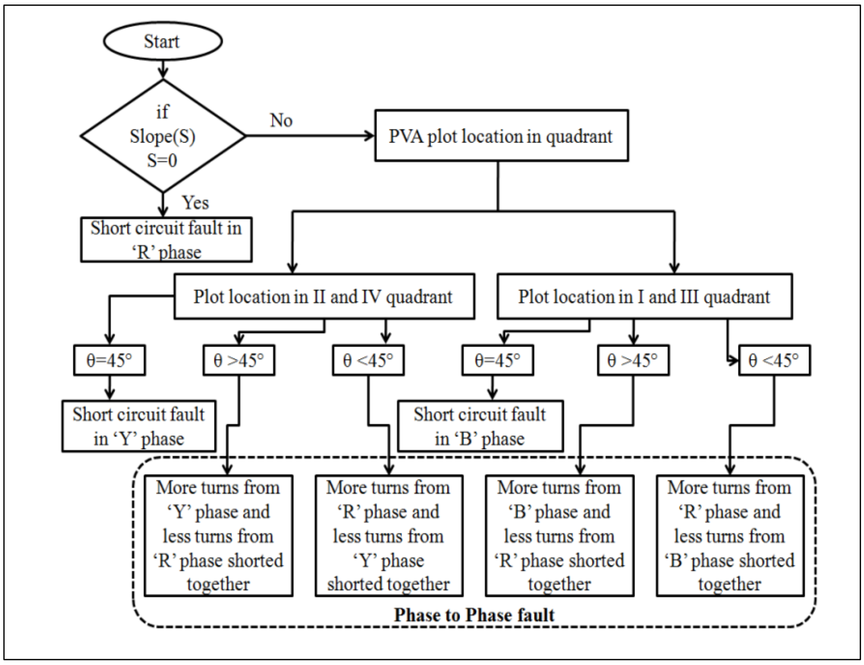

Figure 3 Winding fault detection in electrical machines using PVA

1.2.2. Peak Variation Response (PVR)

In this electrical monitoring technique, fault detection is based on tracing the Peak Variation Response through spectral analysis of electrical signals obtained from electrical machines. In this thesis, the spectrum of current signal and flux signal is analyzed by using peak variations to identify the faults. Generally, oscilloscopes have been used to acquire the electrical signals varying with time. But this information is insufficient to know the fault frequency of electrical signal. To fully understand the performance of an electrical machine or a system, a signal (or signals) must also be analyzed in the frequency domain. In the spectrum analysis the magnitude of an input electrical signals namely, current and flux is measured with respect to frequency.

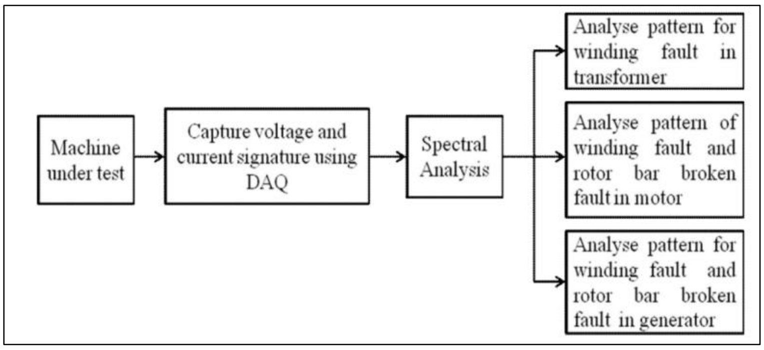

Figure 4 Depicts the scheme for Peak Variation Response (PVR) that is used to diagnose the condition of machine under test

1.2.3. Standard Deviation Technique in Fast Statistics Tool

In Standard Deviation technique, the output electrical signal from faulty machine is collected and given as input into the Fast Statistics tool, where the results of statistical measures such as standard deviation, mean and variance are obtained. These values are compared with the corresponding values of healthy machine and the variation in values with the healthy machine describes the extent of fault occurred in an electrical machine. Among these the standard deviation provides interesting metric of machine fault nature.

2. Techniques used for machine fault detection

The following sections discuss the techniques used in motor fault detection during simulation studies with the magnet software. Here 3ĭ, 415V, 50Hz, 4 pole, 2HP induction machine healthy and faulty condition has been designed using Infolytica MagNet 6.11.2 software. The current data and flux linkage data has been collected from the simulated model and it has been analyzed using Park Vector Approach (PVA), Peak Variation Response and Standard deviation.

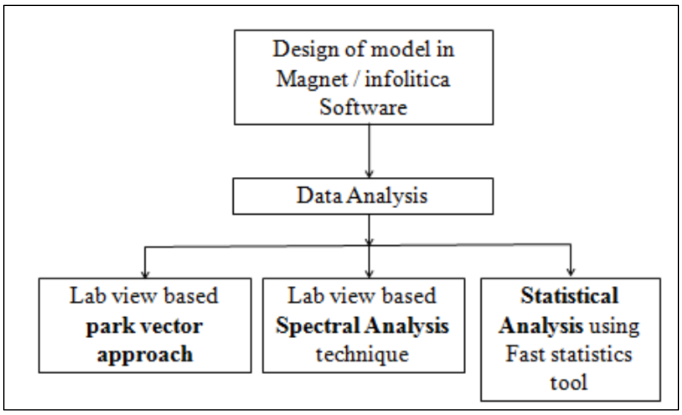

Figure 5 Simplified fault detection block diagram for Induction machine

3. Current monitoring

The designed three phase induction motor using MagNet software has been deliberately fault by creating short circuit in stator winding turns and then simulating to analyze the winding fault. The motor model with different types of winding fault is allowed to run for 5-6 hrs. The flux data, current data and corresponding speed data has been collected for each type of fault.

The induction motor with healthy and winding fault condition has been described by analyzing Peak Variation Response. In this analysis the variations of peak in the spectral form and the side lobe of the spectral peak have been analyzed. The FFT based power spectrum is also using LabVIEW program.

3.1. Peak Variation Response (PVR)

Winding faults have similarity for phase-to-phase short circuit and coil to coil short circuit but, coil to coil short circuit has dominant peaks in multiples of 50Hz. Inter – turn short circuit fault has multiple side lobes for each of harmonic peaks compared to healthy coil.

The flux linkage and current spectral of the winding fault has been described in Figure 6 and Figure 7 respectively. The wave form shape of the Figure 6 and Figure 7 depict the spectral response of the flux linkage data and current data. These two spectral natures are same.

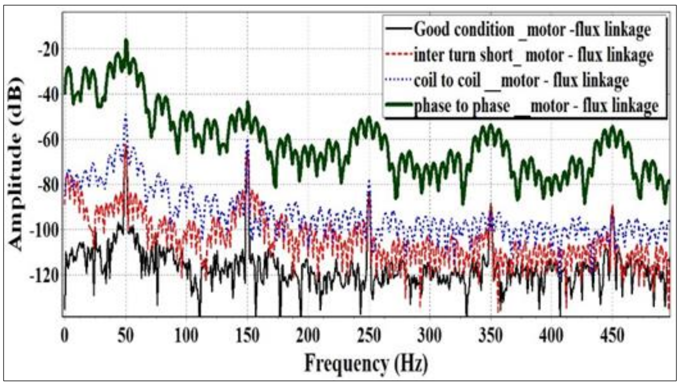

Figure 6 PVR of the flux linkage for winding fault of induction motor

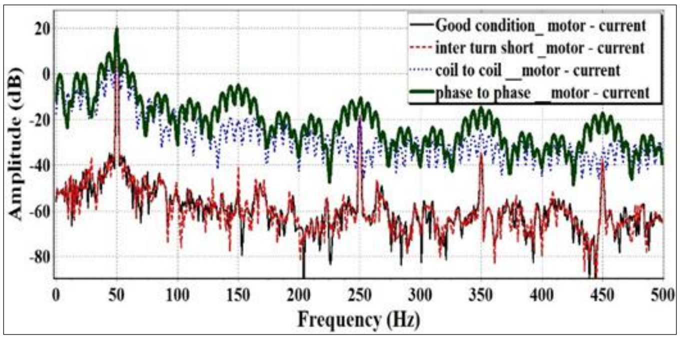

Figure 7 PVR of the current for winding fault of induction motor

The motor speed and fault frequency of the winding fault has been shown in Table 1. From the results it was observed that as the speed of motor falls as fault severity increases the side band lobes for the fundamental frequency 50Hz also tend to decrease closer to main lobe than the expected 25Hz and 75 Hz values.

Table 1 Fault frequency of winding faults in simulation

Machine condition	Speed Nr (rpm)	slip	short circuit fault frequency at (k=1&n=1)		observations
			LSB(Hz)	RSB(Hz)	
Good condition	1500	0	25	75	fo-25Hz to fo+25Hz for normal
Inter – turn short circuit	1260	0.16	29	71	LSB & RSB side lobes shift to FoSpeed decreases by 25%
Coil to coil short	780	0.48	37	63	LSB & RSB side lobes shift to Fo Speed decreases by50%
Phase to Phase short	420	0.72	43	57	LSB & RSB side lobes very close to Fo Speed decreases by 70%

Fault frequency of winding fault listed in Table 1 is same for both current and flux linkage data.

3.2. Park Vector Approach (PVA)

PVA is one of the fault detection techniques in any three-phase machine. In this technique, the instantaneous phase currents of the stator are transformed into Park's vector using equations (3.1) and (3.2). The Equations (3.3) and (3.4) are no longer valid, consequently the observed PVA plot differs from the reference pattern. The fault diagnosis is based on identifying the appearance of an elliptic pattern, corresponding to the motors supply current Park's Vector representation, whose ellipticity increases with the severity of the fault and whose major axis orientation is associated to the faulty phase. The operating philosophy of the Park's Vector Approach is thus based on identifying unique signature patterns in the Figures obtained, corresponding to the machines' current Park's Vector representation. But in the present research work using this method were able to identify fault severity or turns affected by fault in the phase-to-phase fault. It has been illustrated in Figure 8.

$$I_d = \sqrt{\frac{2}{3}} I_r - \sqrt{\frac{1}{6}} I_y - \sqrt{\frac{1}{6}} I_b \text{ ....(3.1)}$$

$$I_q = \sqrt{\frac{1}{2}} I_y - \sqrt{\frac{1}{2}} I_b \text{ ....(3.2)}$$

$$I_d = \frac{\sqrt{6}}{2} I_M \sin(\dot{A}t) \text{ .....(3.3)}$$

$$I_q = \frac{\sqrt{6}}{2} I_M \sin(\dot{A}t-) \text{ .... (3.4)}$$

- Good Coil has PVA as circular plot
- Coil to coil fault in R Phase has PVA as elliptical plot
- Inter – turn fault has PVA with 'a' value higher than 'b' (as per figure 2.5)

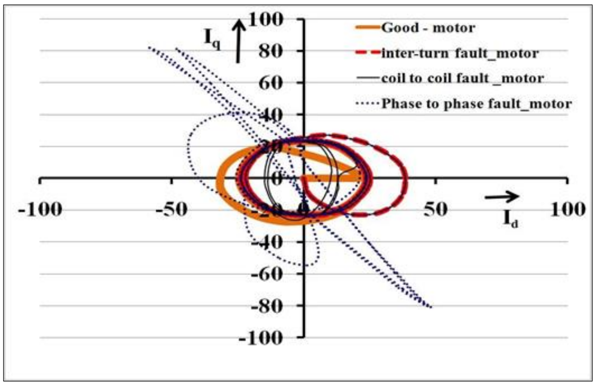

Figure 8 PVA of motor winding fault – simulation

Phase to phase fault: The PVA of phase-to-phase short circuit fault has been lying in 2nd and 4th quadrant. Their slope from the I_d current axis is not equal to'1' (i.e., tangential angle ɧ<45°). It is nothing but more turns from R phase and less turn from Y phase getting shorted.

3.3. Standard Deviation

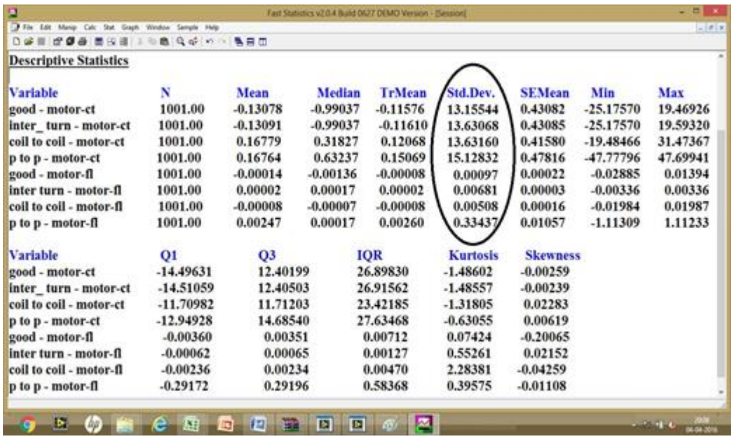

Descriptive Statistics

Variable	N	Mean	Median	TrMean	Std.Dev.	SEMean	Min	Max
good - motor-ct	1001.00	-0.13078	-0.99037	-0.11576	13.15544	0.43082	-25.17570	19.46926
inter_ turn - motor-ct	1001.00	-0.13091	-0.99037	-0.11610	13.63068	0.43085	-25.17570	19.59320
coil to coil - motor-ct	1001.00	0.16779	0.31827	0.12068	13.63160	0.41580	-19.48466	31.47367
p to p - motor-ct	1001.00	0.16764	0.63237	0.15069	15.12832	0.47816	-47.77796	47.69941
good - motor-fl	1001.00	-0.00014	-0.00136	-0.00008	0.00097	0.00022	-0.02885	0.01394
inter turn - motor-fl	1001.00	0.00002	0.00017	0.00002	0.00681	0.00003	-0.00336	0.00336
coil to coil - motor-fl	1001.00	-0.00008	-0.00007	-0.00008	0.00508	0.00016	-0.01984	0.01987
p to p - motor-fl	1001.00	0.00247	0.00017	0.00260	0.33437	0.01057	-1.11309	1.11233

Variable	Q1	Q3	IQR	Kurtosis	Skewness
good - motor-ct	-14.49631	12.40199	26.89830	-1.48602	-0.00259
inter_ turn - motor-ct	-14.51059	12.40503	26.91562	-1.48557	-0.00239
coil to coil - motor-ct	-11.70982	11.71203	23.42185	-1.31805	0.02283
p to p - motor-ct	-12.94928	14.68540	27.63468	-0.63055	0.00619
good - motor-fl	-0.00360	0.00351	0.00712	0.07424	-0.20065
inter turn - motor-fl	-0.00062	0.00065	0.00127	0.55261	0.02152
coil to coil - motor-fl	-0.00236	0.00234	0.00470	2.28381	-0.04259
p to p - motor-fl	-0.29172	0.29196	0.58368	0.39575	-0.01108

Figure 9 Statistical report of motor winding fault-simulation

In the Figure 9 the standard deviation has shown by marking as the main focus is on the values of standard deviation. According to the equation (3.5) the standard deviation is proportional to the magnitude of data observed from the machine. Under short circuit fault condition, the current taken by the machine is always high compare with healthy condition. Therefore, the standard deviation magnitude increases as fault occurs in the machine. Hence by assigning the healthy machine standard deviation value as reference, it is possible to predict that the machine is subject to fault. where,

$$\mathrm{SD} = \sqrt{\frac{1}{N-1}\sum_{i=1}^{N}|A_i-\mu|^2} \quad \ldots\ldots\ldots\ldots\ldots (3.5)$$

where,
SD Standard Deviation
A_i data observed from the simulation and experimental test bed
μ mean value of observed data's
N Number of data's

$$\mu = \frac{1}{N}\sum_{i=1}^{N} A_i \quad \ldots\ldots\ldots\ldots (3.6)$$

$$RMS = \sqrt{\frac{1}{N}\sum_{i=1}^{N}|A_i|^2} \text{ ....(3.7)}$$

- Good - motor-ct Current data of the good motor
- Inter turn - motor-ct Current data of the inter – turn short circuit motor
- Coil to coil – motor-ct Current data of the coil-to-coil short circuit motor
- P to P – motor-ct Current data of the phase-to-phase short circuit motor
- Good - motor-fl Flux linkage data of the good motor
- Inter_turn - motor-fl Flux linkage of the inter – turn short circuit motor
- Coil to coil –motor-fl Flux linkage of the coil-to-coil short circuit motor
- P to P – motor-fl Flux linkage data of the phase-to-phase short circuit

Standard Deviation value increases as fault severity increases. Therefore, Standard Deviation value for good coil <inter turn<coil to coil <phase to phase fault.

4. Flux pattern analysis

To identify the winding fault in the induction motor, the flux data is used in the form of flux pattern. The prototype induction motor has been designed with taps on the stator winding to create winding faults.

In the present research work discussions are based on inter turn short circuit fault created in R phase' first coil at its middle turns. The coil-to-coil short fault has been created within two coils of the R phase. Similarly, the phase-to-phase short circuit is introduced across R phase coil and Y phase coil. The above-mentioned winding failures are implemented stator winding of the induction motor. The stator winding is connected in star connection. Each phase carries 4 coils. The short circuit fault is designed by short circuiting the turns with switch S. Then flux linkages at the short-circuited portions has been captured and analyzed.

The three-phase induction motor model has been analyzed at noload under healthy and faulty condition by using transient 2D solver in MagNet 6.11.2. The stator winding of the induction motor has been subjected to various faults such as inter-turn short circuit, coil to coil short and phase-tophase fault. The fault is created by closing the switch at 208ms (i.e., after 10 cycles) of total simulation time. After that, it has been opened with few milliseconds delay time. This fault has been reflected in the flux path of the motor model. The flux pattern has been captured at 208ms from the simulated model. At 208ms the uniform flux pattern has been observed in the fault free motor. It is shown in Figure 10. The flux is diverging from one tooth and converging to other teeth as per the winding wounded in the teeth. The magnetic field distribution in induction motor under healthy condition is symmetrical.

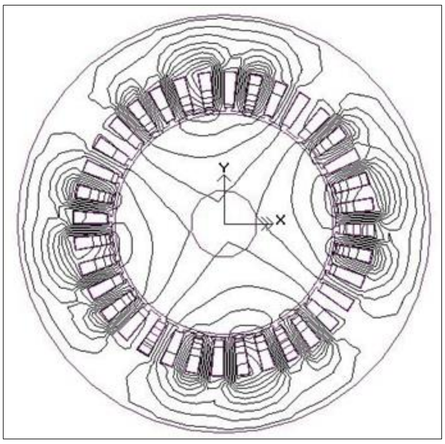

Figure 10 Flux pattern of the motor in healthy condition

Inter – turn winding fault shows the flux concentric in the fault pole compare to other poles and it spreads over a larger area. It is shown in Figure 11. The short circuit has occurred in middle portion of first coil of R phase of the motor subjected to fault. In this simulated design, the flux has concentric in the portion of the winding subjected to short circuit, as pointed by red circle in Figure 11. below.

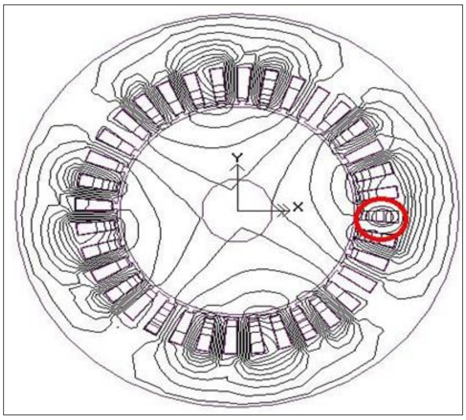

Figure 11 Flux pattern of the motor subjected to inter turn short circuit fault

In this coil to coil fault model, the flux dense on the stator core and non-observed in the rotor. It is shown in Figure 12. The motor is simulated under this coil to coil short circuit fault condition. Generally in healthy condition, the flux induced in the stator is entering in to the rotor through air gap.

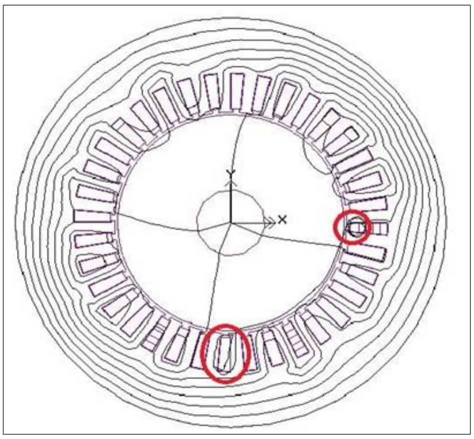

Figure 12 Flux pattern of the motor subjected to coil to coil short circuit fault

But in this simulated model no flux observed in rotor. So it is identified as coil to coil fault model. This affected flux circulated in the R phase coil which was indicated by circle in Figure 12. The affected portion is belonging to R phase coil. Hence the coil to coil short circuit fault is occuring in R phase.

The simulated model of phase-to-phase fault has been shown in Figure 13. The flux lines are absent in the stator core and rotor bar. However, the circulating weak flux was observed at the location of short circuit coils emanating from R phase to Y. The circulated flux in the affected coil is pointed by red circle in Figure 13. This affected coil is belonging to R phase and Y phase coil. Hence phase(R) to phase(Y) fault has been identified.

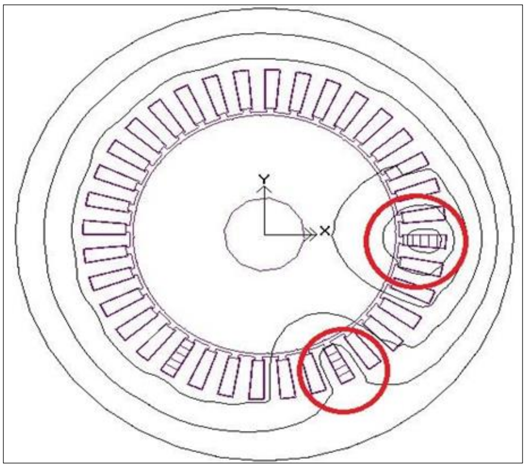

Figure 13 Flux pattern of the motor subjected to Phase to phase short circuit fault

But the asymmetrical distribution of magnetic flux linkage has observed in winding fault conditions.

4.1. Experimental results for winding fault diagnosis

The Figure 14 shows the block diagram of experimental set-up for induction machine module. The three phase supply has been given to Induction machine. The stator winding current is acquired through DSO using current probe. The acquired data signal is fed to LabVIEW software for detecting fault with park vector approach and Peak Variation Response. The fast statistics tool has been used to validate fault by standard deviation.

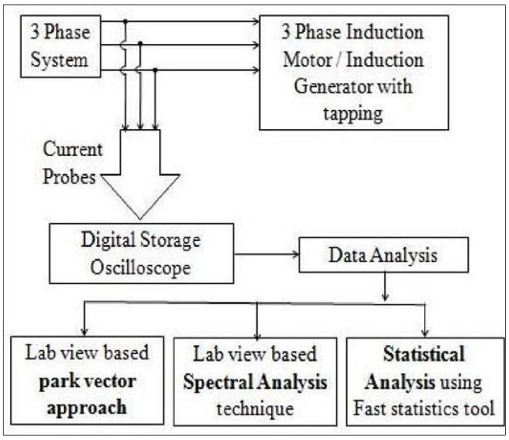

Figure 14 Simplified Experimental block diagram for Induction machine

4.1.1. Analysis using peak variation response (PVR)

The three phase squirrel cage induction motor has been rotating with decreasing speed under winding fault condition (i.e.,) from 1500rpm (Good condition) to 1260rpm (inter – turn short circuit fault) and 720rpm (phase to phase short circuit fault). The theoretical calculation of the motor under winding fault has shown in Table4.1. This calculation is performed by Equation (4.1).

$$f_{sc} f_1 \left(k \; r \; \_\_ np \; (1 \; s) \right) \quad \text{.............} \; (4.1)$$

P - Pole pairs
s - Rotor slip
k-1, 3, 5...
f1 - Fundamental frequency (Hz)
fsc -Frequency components of the current due to stator winding fault (Hz)
n- Integer 1, 2, 3…

Table 2 Fault frequency for winding faults based on empirical formula

Machine condition	Rotor speed N_r(rpm)	slip	n	Short circuit fault frequency (f_{sc})					
				K=1 50Hz		K=3 150Hz		K=5 250Hz	
				LSB	RSB	LSB	RSB	LSB	RSB
Good condition	1500	0	1	25	75	125	175	225	275
			2	0	100	100	200	200	300
			3	25	125	75	225	175	325
			4	-50	150	50	250	150	350
			5	-75	175	25	275	125	375
inter– turn short circuit fault	1260	0.16	1	29	71	129	171	229	271
			2	8	92	108	192	208	292
			3	-13	113	87	213	187	313
			4	-34	134	66	234	166	334
			5	-55	155	45	255	145	355
phase to phase short circuit fault	720	0.52	1	38	62	138	162	238	262
			2	26	74	126	174	226	274
			3	14	86	114	186	214	286
			4	2	98	102	198	202	298
			5	-10	110	90	210	190	310

where, LSB- Left Side Band & RSB- Right Side Band

In Equation, the 'n' and 'K' has assumed as n=1, 2, 3, 4 and 5.

K=1, 3 and 5

The side lobes seem to tend to shrink more towards the corresponding peak frequencies and the observation is that, this variation is more for phase to phase short circuit fault>inter– turn short circuit fault>Good condition side lobes

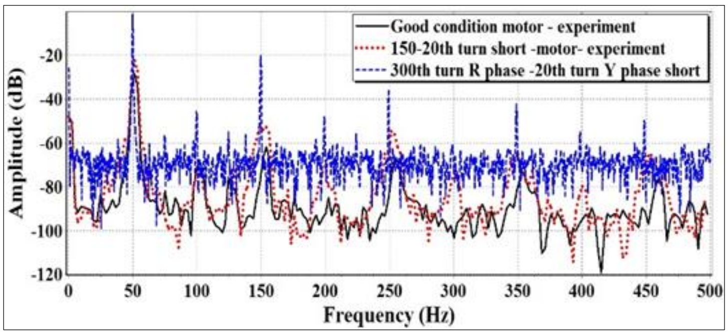

Figure 15 PVR for winding fault of induction motor full view - experiment

The Peak Variation Response of the experimental current data of the winding fault is as shown in Figure 15.

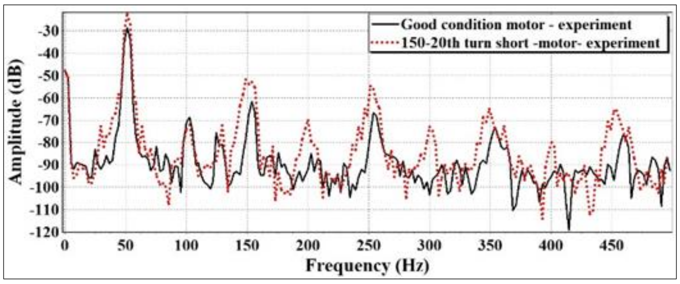

Figure 16 PVR for Good and Inter – turn short circuit fault full view - experiment

Good condition, Inter – turn fault and Phase to phase short circuit fault condition, the harmonic peaks are obtained in the order of 50Hz>150Hz> 250Hz >350Hz>450Hz

The side lobes seem to tend more towards the corresponding peak frequencies:

Phase to phase short circuit fault>inter– turn short circuit fault>Good condition side lobes. It is verified from Table 3.

Table 3 Fault frequency for experimental winding faults

Machine condition	**Speed (rpm)**	**Slip**		**N=1**		
			K=1 (at 50Hz)		K=3 (at 150Hz)	
			Short circuit fault frequency(Hz)		Short circuit fault frequency(Hz)	
			LSB	RSB	LSB	RSB
Good condition	1450	0	25.83	74.16	125.83	174.16
Inter – turn short	1260	0.16	29.29	70.80	129.3945	170.8984
Phase to Phase fault	720	0.52	38.32	62.9	137.902	162.066

4.1.2. Analysis using park vector approach (PVA)

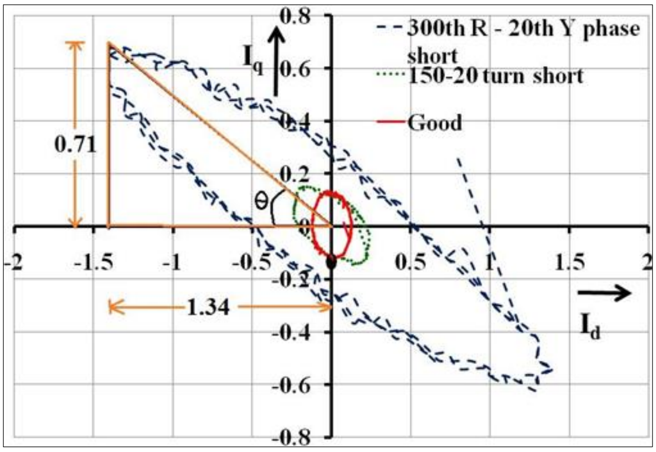

Figure 17 PVA of winding fault – experiment

In phase to phase short circuit fault, 300th turn in R phase and 20th turn in Y phase are subjected to short circuit. The tangential angle is 28.072°. The fault nature is reflected in angle. i.e., the short circuit fault in R phase is reflected by approximately 0°. The short circuit fault in Y phase is reflected by approximately 45°. But tangential angle obtained from phase to phase fault is 28.072°. Hence, the fault is not R phase fault and neither Y phase fault; it is verified as R phase to Y phase fault. The tangential angle of inter – turn short circuit fault is approximately 45°. Hence, it is referred as inter – turn fault in Y phase.

4.1.3. Standard Deviation

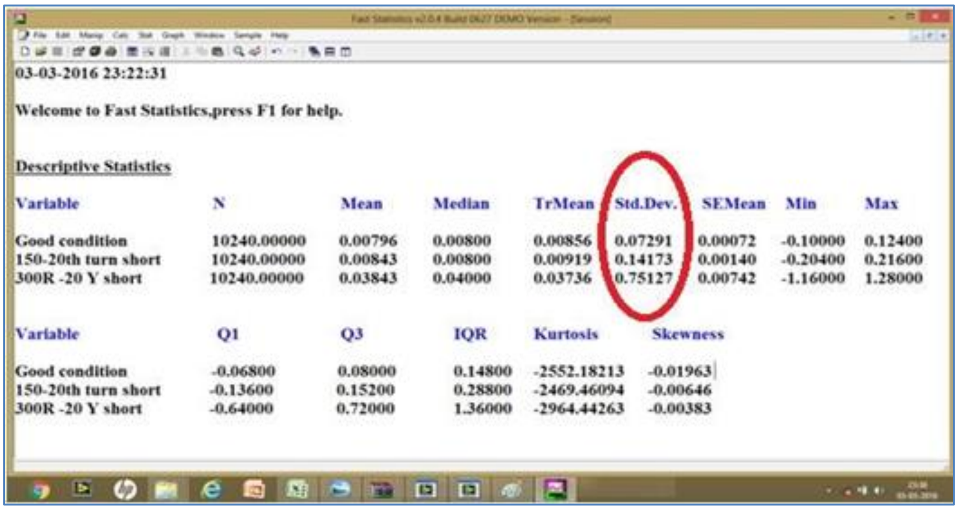
03-03-2016 23:22:31

Welcome to Fast Statistics,press F1 for help.

Descriptive Statistics

Variable	N	Mean	Median	TrMean	Std.Dev.	SEMean	Min	Max
Good condition	10240.00000	0.00796	0.00800	0.00856	0.07291	0.00072	-0.10000	0.12400
150-20th turn short	10240.00000	0.00843	0.00800	0.00919	0.14173	0.00140	-0.20400	0.21600
300R -20 Y short	10240.00000	0.03843	0.04000	0.03736	0.75127	0.00742	-1.16000	1.28000

Variable	Q1	Q3	IQR	Kurtosis	Skewness
Good condition	-0.06800	0.08000	0.14800	-2552.18213	-0.01963
150-20th turn short	-0.13600	0.15200	0.28800	-2469.46094	-0.00646
300R -20 Y short	-0.64000	0.72000	1.36000	-2964.44263	-0.00383

Figure 18 Statistical report of winding fault

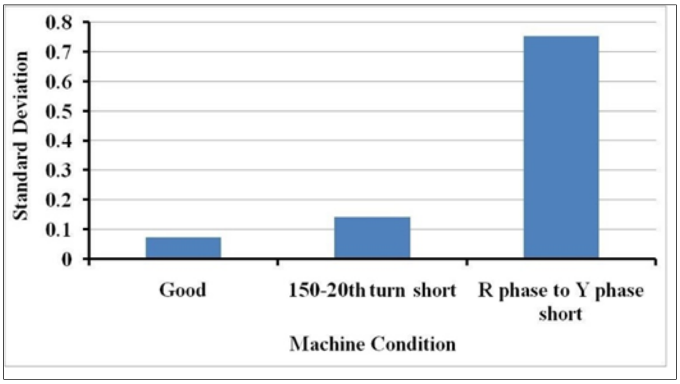

Figure 19 Standard deviation of the winding fault

Figure 4.7 and Figure 4.8 shows that the standard deviation of 150 – 20th turn short (inter – turn short) is two times the standard deviation of the good condition motor. But the phase to phase fault as ten times the standard deviation of the good condition motor. Therefore phase to phase fault is proved as severe fault compare to inter – turn short circuit fault.

4.1.4. Artificial Intelligince on finding the fault

Artificial neural network (ANN): This is a technique that mimics the structure and function of biological neurons to learn from data and perform tasks such as classification, regression, clustering, etc. ANN can be used to classify different types of motor faults based on the features extracted by PVR and PVA. E.g. a multilayer perceptron (MLP) network to classify stator winding faults, rotor bar faults, and bearing faults based on the PVR and PVA features of the stator current signals.

Support vector machine (SVM): This is a technique that finds the optimal hyperplane that separates the data into different classes with maximum margin. SVM can be used to classify different types of motor faults based on the features extracted by PVR and PVA E.g. a radial basis function (RBF) kernel SVM to classify stator winding faults, rotor bar faults, bearing faults, and eccentricity faults based on the PVR and PVA features of the stator current signals.

Random forest (RF): This is a technique that combines multiple decision trees to form an ensemble classifier that can improve the accuracy and robustness of the prediction. RF can be used to classify different types of motor faults based on the features extracted by PVR and PVA. E.g. RF to classify stator winding faults, rotor bar faults, bearing faults, and eccentricity faults based on the PVR and PVA features of the stator current signals.

Standard deviation (SD): This is a technique that measures the variation or dispersion of a set of values from their mean. SD can be used to select the most relevant features that can discriminate between different fault types and healthy conditions. E.g. SD to select the best features from PVR and PVA for fault classification using ANN, SVM, and RF.

Results derived between SD, PVR and PVA as follows,

Table 4 Condition Monitoring of Electrical Machines

Faulty condition in Machine New contribution in Machine condition monitoring techniques	**New contribution in Machine condition monitoring techniques**
Squirrel cage Induction machine(motor/generator) winding fault	PVA: The slope of the plot is be used to identify the faulty phase for a machine (motor/generator) with stator winding fault. In phase-to-phase fault, the nature of short-circuited turns in each phase is identified shown in Figure 3. PVR: spectral peak occurs only at odd odder frequency (50Hz, 150Hz, 250Hz...) The fault severity increases, side lobe move towards the main peak. At severe fault condition like phase-to-phase faulty spectrum has multiple projected side lobes on both LSB and RSB of every odd odder harmonic. Also, observed that 2 sets of multiple projected side lobes occurs between each odd odder harmonic peak of motor and 3 sets of side lobes occurs between each odd odder harmonic peak in case of fault in generator. The analysis of PVR scheme as shown in Figure 4. SD: As the fault severity increases the SD also increases

5. Conclusion

Condition monitoring (CM) has become a very important technology in the field of electrical machine maintenance, and has attracted more and more attention worldwide. The potential functions of failure prediction, detection, machine fault identification, and aging estimation bring a series of advantage for utility companies by reducing maintenance cost, incorporating early maintenance procedures onto machines, enhancing safety of operators, minimizing accident and the severity of damages, as well as improving power quality. Due to these benefits and the pressure to utilize the existing assets under a environment of multiple machines of various configurations functioning in large scale grids or industries, condition monitoring is now a valuable domain of interest to power system managers and engineers as well as researchers.

This work has focused on condition monitoring and fault diagnosis of three-phase squirrel cage induction machines as generators and motors using signal processing approaches such as analysis of peak variation response (PVR), Park Vector Approach (PVA) and with statistical analysis using standard deviation (SD).

References

[1] Zhang, Z., Wang, X., Wang, Y., & Xu, D. (2021). An overview of artificial intelligence applications for power electronics. IEEE Transactions on Power Electronics, 36(4), 4633-4658

[2] Kumar, S., & Kumar, A. (2020). Artificial intelligence in the field of electrical engineering. International Journal of Engineering Research and Technology (IJERT), 9(10), 7-10

[3] Sukhjeet Singh and Navin Kumar, 2017, 'Detection of Bearing Faults in Mechanical Systems Using Stator Current Monitoring' IEEE Transactions on Industrial Informatics, vol. 13, no. 3, pp.1341-1349.

[4] Tavner, PJ & Penman, J 1987, 'Condition monitoring of electrical machines', Research Studies Pre, vol. 1.

[5] Thomas, VV, Vasudevan, K & Kumar, VJ 2002, 'Implementation of online air-gap torque monitor for detection of squirrel cage rotor faults using TMS320C31', International Conference on Power Electronics, Machines and Drives, (Conf. Publ. No. 487), IET, pp. 128-132.

[6] Trzynadlowski, AM & Ritchie, E 2000, 'Comparative investigation of diagnostic media for induction motors: a case of rotor cage faults', IEEE Transactions on Industrial Electronics, vol. 47, no. 5, pp. 1092-1099.

[7] Wang, H & Butler, KL 2001, 'Finite element analysis of internal winding faults in distribution transformers', IEEE Transactions on Power Delivery, vol. 16, no. 3, pp. 422-428.

[8] Sahoo, A., & Panda, G. (2019). Fault diagnosis of induction motor using artificial intelligence techniques: a review. International Journal of System Assurance Engineering and Management, 10(5), 1041-10581

[9] Dhashanamoorthi, Balaji. Opportunities and Challenges of Artificial Intelligence in Banking and Financial services.

[10] Dhashanamoorthi, Balaji. Artificial Intelligence in combating cyber threats in Banking and Financial services.

[11] Kumar, R., & Singh, B. (2017). Fault diagnosis of electrical machines using artificial intelligence techniques: a review. International Journal of Engineering and Technology, 9(4), 2790-2798.

[12] Singh, A., & Singh, B. (2016). Artificial intelligence based fault diagnosis of electrical machines: a review. International Journal of Engineering and Technology, 8(6), 2523-2531.

[13] Li, Y., Zhang, Y., & Wang, Z. (2020). Fault diagnosis of electrical machines based on deep learning: A review. IEEE Transactions on Industrial Electronics, 67(8), 6668-66781

[14] Dhashanamoorthi, Balaji. Artificial Intelligence to detection fault on three phase squirrel cage induction motors subjected to broken bar fault (2023).

[15] Dhashanamoorthi, Balaji. Fault Detection and Identification in Three Phase Transformer using AI based FSA and PVR analysis (2023).

[16] Dhashanamoorthi, Balaji. EFFICIENCY IMPROVEMENT ON WIND TURBINE THROUGH BUMP UP STEPPER MOTOR (2022).

[17] Dhashanamoorthi, Balaji. Construction of suffix tree using key phrases for document Using down-top incremental conceptual hierarchical text clustering approach (2022).